Contractile responses of smooth muscle cells differentiated from rat neural stem cells

Kazuhiko Oishi, Yasuhiro Ogawa, Shuji Gamoh and Masaatsu K. Uchida

Department of Pharmacology, Meiji Pharmaceutical University, Tokyo 204-8588, Japan

To characterize the functional differentiation of neural stem cells into smooth muscle cells, multipotent stem cells in the central nervous system (CNS) were isolated from rat embryonic day 14 (E14) cortex and cultured by neurosphere formation in serum-free medium in the presence of 10 ng ml^{-1} of basic fibroblast growth factor. Differentiation was induced by the addition of 10 % fetal bovine serum to low-density cultures (2.5×10^3 cells cm^{-2}). Immunological analyses and reverse transcriptase-polymerase chain reaction indicated that the differentiated cells expressed smooth-muscle-specific marker proteins such as SM-1, SM-2, and SMemb myosin heavy chains, SM-22, basic calponin and α-smooth-muscle actin, but not the astrocyte marker glial fibrillary acidic protein. To examine whether smooth-muscle-like cells that are differentiated from CNS stem cells possess the characteristics of contractile smooth muscle, we prepared reconstituted collagen gel fibres and measured their contractile tension. The reconstituted fibres were prepared by thermal gelation of collagen and the differentiated cells. The fibres contracted in response to treatment with KCl (80 mM), ACh (100 μM), endothelin-1 (10 nM), endothelin-2 (10 nM), and prostaglandin F2α (100 μM). ACh-induced contraction was partially inhibited by the L-type voltage-dependent Ca^{2+} channel inhibitor nifedipine and by the intracellular Ca^{2+} chelator 1,2-bis (2-aminophenoxy) ethane-*N,N,N´,N´*-tetraacetic acid acetoxymethyl ester, the myosin light chain kinase inhibitor ML-9, the Rho kinase inhibitor Y-27632, dibutyryl cAMP and 8-bromo-cGMP. These results suggest that CNS stem cells give rise to smooth muscle cells *in vitro* that have an identical contractile function to smooth muscle *in vivo*.

(Received 17 September 2001; accepted after revision 13 January 2002)

Corresponding author K. Oishi: Department of Pharmacology, Meiji Pharmaceutical University, 2-522-1, Noshio, Kiyose, Tokyo 204–8588, Japan. Email: oishikz@my-pharm.ac.jp

Multipotent stem cells that can generate neurones and glial cells exist in various regions of the vertebrate central nervous system (CNS) during development. A small number of the stem cells are also present in the adult CNS, although their ability to generate new cells in response to injury or degenerative disease has not been demonstrated. Mujtaba *et al.* (1998) have shown that CNS stem cells isolated from rat embronic days 105–13.5 (E10.5–E13.5) spinal cord give rise to large, flat, smooth-muscle-like cells that express α-smooth-muscle actin, a marker characteristic of smooth muscle cells and smooth-muscle-related cells. A recent study by Tsai & McKay (2000) using CNS stem cells isolated from the rat E14 cortex also showed an unexpected differentiation into smooth-muscle-like cells that expressed α-smooth-muscle actin, SM-22 and basic calponin. These findings indicate that CNS stem cells have the capacity to turn into smooth-muscle-like cells and are much more plastic than previously thought. Although the significance of the CNS stem cell origin of smooth muscle cells in physiological and pathological states needs to be evaluated, it is possible that smooth muscle cells are in part derived from CNS stem cells.

Smooth muscle cells are highly specialized cells whose principal function is contraction. The terminally different-iated or mature smooth muscle cell proliferates at an extremely low rate and expresses a unique repertoire of contractile proteins, contractile agonist receptors, ion channels and signalling molecules, which are required for its contractile function. In the studies of Mujtaba *et al.* (1998) and Tsai & McKay (2000), the differentiation of CNS stem cells into smooth-muscle-like cells was demonstrated only by immunocytochemical analyses and reverse transcriptase-polymerase chain reaction (RT-PCR) experiments. It is unclear, however, whether these cells possess contractile ability and respond to contractile stimuli. We have recently established a method for reconstituting artificial smooth muscle fibres (Oishi *et al.* 2000). This method permits for the first time the quantitative measurement of the contractile force generated by smooth muscle cells of a defined type, and enables us to make direct observations of the contractile function of those differentiated cells. In the present study, we have shown for the first time that smooth-muscle-like cells that are differentiated from CNS stem cells exhibit a

contractile function that is identical to that of smooth muscle *in vivo*.

METHODS

Isolation and propagation of CNS stem cells

All procedures using animals were performed in accordance with the Guidelines for Animal Experimentation of the Japanese Association for Laboratory Animal Science, and were approved by the Institutional Animal Use and Care Committee at Meiji Pharmaceutical University. CNS stem cell culture was performed as described by Gritti *et al.* (1996) with minor modifications. Briefly, pregnant Sprague-Dawley rats (Charles River) at gestational day 14 were anaesthetized by intraperitoneal injection of pentobarbital (35 mg kg^{-1}) and exsanguinated. Embryos were removed and placed in a Petri dish containing Hanks' balanced salt solutions (HBSS). After decapitation, the brain was removed. The cortex was dissected out and carefully triturated with a fire-polished Pasteur pipette in N2 medium in the presence of 10 ng ml^{-1} basic fibroblast growth factor (bFGF) and 2 μg ml^{-1} heparin. Cells were collected by centrifugation for 1 min at 10 g and resuspended in N2 medium. Viable cells were plated in 60 mm Petri dishes (Corning, NY, USA) at 10^5 cells ml^{-1} in N2 medium, and were maintained at 37 °C in 5 % CO$_2$–95 % air. The number of primary spheres generated was assessed 2–3 days after plating. Spheres were collected by centrifugation for 5 min at $450 \times g$ and dissociated mechanically to single-cell suspensions. Some cells were processed for immunocytochemistry and the remainder were replated at 10^5 cells ml^{-1} in fresh N2 medium with bFGF. By 3–4 days after plating, new spheres were formed that could undergo further passage (Fig. 1*B*, *C*). Cultures of up to five passages were used.

Differentiation of CNS stem cells

Spheres (passages 2–5) were dissociated mechanically to single-cell suspensions and replated onto poly-L-ornithine–fibronectin-coated glass coverslips or culture dishes at different cell densities (2.5×10^3, 5×10^3 and 10^5 cells cm^{-2}). Undifferentiated CNS stem cells were then cultured for 7 days with 10 % fetal bovine serum (FBS) after bFGF withdrawal.

Antibodies used

Anti-rat nestin (no. 130) is a rabbit polyclonal antibody specific for nestin. This antibody was kindly provided by Dr McKay (Tsai & McKay, 2000). The anti-α-smooth-muscle isoform of actin is a monoclonal antibody raised against a synthetic NH$_2$ terminal decapeptide of the smooth muscle α-isoform of actin (Progen Biotechnik, Germany). Anti-SM-1 (clone 1C10), SM-2 (clone 2B8) and SMemb (clone 3H2) are monoclonal antibodies that recognize specifically the SM-1, SM-2 and SMemb isoforms of smooth muscle myosin heavy chains, respectively (Yamasa, Japan). Anti-MAP2 (clone HM-2) is an IgG1 monoclonal antibody specific for MAP2. Anti-glial fibrillary acidic protein (GFAP) is a rabbit polyclonal antibody raised against GFAP purified from bovine spinal cord (Dako, CA, USA). Anti-5-bromo-2′-deoxyuridine (BrdU) is a monoclonal antibody specific for BrdU (Boehringer-Mannheim, Germany). Biotinylated anti-mouse and anti-rabbit IgG secondary antibodies raised in horse and goat, respectively, were from Vector Laboratories (CA, USA). A fluorescein-conjugated anti-mouse IgG secondary antibody raised in goat was from Tago (CA, USA). An R-phycoerythrin (R-PE)-conjugated anti-rabbit IgG secondary antibody raised in goat was from Southern Biotechnology Associates (AL, USA).

Immunocytochemistry

Cultures grown on poly-L-ornithine–fibronectin-coated glass coverslips were washed with phosphate-buffered saline (PBS; 137 mM NaCl, 2.7 mM KCl, 4.3 mM Na$_2$HPO$_4$·7H$_2$O and 1.4 mM KH$_2$PO$_4$) for 3 min, fixed in 4 % paraformaldehyde for 15 min and then incubated in PBS containing 0.5 % Triton X-100 for 15 min at room temperature (RT). After fixation, cells were stained at RT for 1 h with one of the following antibodies: anti-nestin (1:50), anti-GFAP (1:10), anti-MAP2 (1:500), anti-α-smooth-muscle actin (1:10), anti-SMemb (1:3000), anti-SM-1 (1:3000), or anti-SM-2 (1:400). The cells were then incubated for 60 min at RT with biotinylated IgG secondary antibodies diluted 1:500 in PBS. This was followed by a second 60 min incubation in avidin-biotin solution (Vectastain ABC Elite kit). Both incubations were preceded by thorough rinsing with PBS. The reaction products were visualized with 3′,3′-diaminobenzidine and hydrogen peroxide (DAB kit). Cells were then washed three times with PBS, and the coverslips were mounted in Permount. Cells were viewed and photographed with the aid of an Olympus photomicroscope. For double-labelled immunofluorescence staining, primary antibodies raised in two different species, anti-GFAP and anti-α-smooth-muscle actin, were incubated together. This was followed by reaction with an appropriate combination of either fluorescein-conjugated anti-mouse IgG antibody (1:500) or R-PE-conjugated anti-rabbit IgG antibody (1:1000). After being washed in water, coverslips were mounted and photographed with the aid of a confocal laser scanning microscope (Olympus, LSM GB-200). Secondary antibody controls were processed simultaneously using the same protocol, except that dilution solutions were devoid of primary antibodies. All secondary controls were negative for staining.

BrdU incorporation

To assess the proliferation of CNS stem cells, BrdU was added to the cells at a concentration of 10 μM and the cells were incubated for 18 h. The cells were then plated onto poly-L-ornithine–fibronectin-coated glass coverslips and incubated for a further 1 h. Next they were washed in PBS and then fixed with 2 % paraformaldehyde for 15 min followed by 95 % methanol for 30 min at −20 °C. Cells were then processed for double-labelled immunocytochemistry using anti-nestin polyclonal antibody and anti-BrdU antibody (following the recommendations of the manufacturer). Antibody labelling was visualized by incubation with fluorescein-conjugated anti-mouse antibody and R-PE-conjugated anti-rabbit antibody for 1 h at RT. After a wash in water, coverslips were mounted and photographed with the aid of a confocal laser scanning microscope.

RT-PCR analysis

Total RNA was isolated from the cells (5×10^5 cells) or the reconstituted fibres (~15 mm in total length) using an Isogen RNA purification kit (Nippon Gene, Tokyo, Japan) according to the manufacturer's protocol. One microgram of total RNA was reverse transcribed using a Superscript preamplification system (Life Technologies, MD, USA) with oligo (dT)12–18 primers (20 μg ml^{-1}) in a 25 μl reaction mixture, according to the manufacturer's protocol. The PCR was performed in 25 μl reaction mixtures using a Perkin-Elmer Thermocycler (Model 9600). Aliquots of the cDNA derived from 50 ng of total RNA were subjected to PCR amplification with primer sets specific to the gene of interest. An initial denaturation for 7 min at 94 °C was followed by 18–35 cycles of denaturation for 30 s at 94 °C, annealing for 30 s at an appropriate temperature, and extension

for 60 s at 72 °C. PCR amplification was followed by a final extension step of 7 min at 72 °C. For each amplification, the number of cycles was chosen such that the amount of reaction products did not reach a plateau. The reaction mixture contained cDNA template, 5′ and 3′ primers each at 0.4 μM, each of the four dNTPs at 200 μM and 1 U of *Taq* polymerase (Takara, Japan), in a buffer containing 10 mM Tris-HCl, 50 mM KCl and 1.5 mM MgCl$_2$. To ensure that the PCR signals detected were not caused by amplification of genomic DNA, control RT-PCR experiments were performed in which cDNA was synthesized without reverse transcriptase. The primers for GAPDH were used as an internal control to confirm that the amount of input RNA was the same for each sample. The oligonucleotide primers used are listed in Table 1. All primers were checked for cross-homology using a DDBJ nucleotide database search (BLASTN) and were determined to be specific for each gene. Primers with minimal secondary structures or a dimmer formation were also checked using the OLIGO software (National Biosciences, MN, USA). The PCR products were resolved in 2 % agarose gels prestained with ethidium bromide (0.5 μg ml^{-1}). They were visualized by ultraviolet transillumination and photographed using 667 Polaroid film.

Semi-quantitative PCR

In order to compare the intensity of the PCR signals between the samples of CNS stem cells and the differentiated cells, the PCR signals for GAPDH were used to normalize the variation in the quantity of cDNA samples. After appropriate variation of the PCR using GAPDH primers, the PCR products were run on 2 % agarose gels and photographed as described earlier. The image of each gel was scanned and exported in a TIFF file, and DNA bands were quantified using NIH Image software (version 1.62). Using this system, the intensity of a known quantity ($\leqslant$ 500 ng) of 100 bp DNA ladder markers (New England Biolabs, MA, USA) was directly proportional to the amount of the DNA present. After the concentration of the specific reaction product was normalized, PCR reactions of cDNA samples in the same volume were performed at different cycle numbers using appropriate primers. The intensities of amplified products were plotted on a graph, and the amount of each DNA band was compared in the linear range for each gene.

Preparation of reconstituted fibres

String-shaped reconstituted collagen gel fibres were prepared using a modification of a method that has been described previously (Oishi *et al.* 2000). Briefly, differentiated cells were suspended in an ice-cold collagen solution containing cultured cells (2.5 × 10^6 cells ml^{-1}), collagen type I-A (2.2 mg ml^{-1}) and collagen type IV (0.24 mg ml^{-1}) in Dulbecco's modified Eagle medium (DMEM, high glucose) supplemented with penicillin (50 U ml^{-1}), streptomycin (50 μg ml^{-1}) and 10 % FBS. An aliquot (0.5 ml) of the collagen-cell suspension was poured into rectangular wells (0.7 × 3.0 × 0.5 cm deep) with two poles placed 2 cm apart on the bottom of each well, and placed in a CO$_2$ incubator (humidified 5 % CO$_2$–95 % air atmosphere) at 37 °C. The collagen gel suspension gelled within 30 min. After 30 min, 5 ml of N2 medium in the presence of 10 % FBS was added to each Petri dish. The preparations were incubated until the cells shrank the gel and formed a string-shaped fibre.

Measurement of isometric force

Fibres prepared as described earlier were mounted vertically in a 10 ml organ bath containing Leibovitz's L-15 medium, pH 7.4, at 37 °C. The fibres were equilibrated in the same medium for 1 h at a resting tension of 1 mN. The tension was recorded isometrically

with a force displacement transducer (TB-612T, Nihon Kohden, Tokyo, Japan). Contractile studies were performed by adding various chemical agents to the final desired concentration or by replacing the medium with potassium-rich solution (80 mM KCl, 59.7 mM NaCl, 1.8 mM CaCl$_2$, 1.0 mM MgCl$_2$, 5.6 mM glucose and 4.2 mM Hepes, pH 7.4 at 37 °C). To observe the calcium dependence of contraction, in some experiments normal and calcium-free, Hepes-buffered Tyrode solutions were used as bathing solutions. The normal solution had the following composition: NaCl 137 mM, KCl 2.7 mM, CaCl$_2$ 1.8 mM, MgCl$_2$ 1.0 mM, glucose 5.6 mM and Hepes 4.2 mM (pH 7.4 at 37 °C). The calcium-free solution had the same composition as normal solution except that CaCl$_2$ was omitted. BAPTA-AM (50 μM) and BAPTA (1 mM) were added to the calcium-free solution for the chelation of cytosolic and extracellular Ca^{2+}, respectively.

Histological observation of sectioned fibres

The collagen gel matrix or fibre including differentiated cells was fixed with freshly prepared 4 % paraformaldehyde in PBS for at least 3 h at 4 °C followed by cryoprotection in 30 % sucrose in PBS at 4 °C for 24–48 h. The gels were immersed in Tissue-Tek O.C.T. (Miles, Elkhart, IN, USA) and frozen in liquid nitrogen. Longitudinal sections (10 μm) were cut using a cryostat. The sections were then subjected to haematoxylin-eosin staining.

Drugs used

Collagen types I-A and IV were purchased from Nitta Gelatin, (Japan); ACh (Ovisot) was from Daiichi Pharmaceutical (Tokyo, Japan); noradrenaline (NA), 5-hydroxytryptamine (5-HT), BAPTA, BAPTA-AM and nifedipine were from Wako Pure Chemicals (Osaka, Japan); ML-9, prostaglandin F2α, endothelin-1, endothelin-2, angiotensin II, dibutyryl cAMP (db-cAMP), 8-bromo-cGMP (8-Br-cGMP), BrdU and the DAB kit were from Sigma Chemical (MO, USA); the Vectastain ABC Elite kit was from Vector Laboratories (CA, USA). Leibovitz's L-15, DMEM was from Gibco RBL (MD, USA). Y-27632 was a generous gift from Yoshitomi Pharmaceutical Industries (Osaka, Japan). All other chemicals were of reagent grade.

Data analysis

All data are presented as means ± S.E.M. Student's *t* tests were used for individual comparisons of contractile tension between groups.

RESULTS

CNS stem cells present in the embryonic rat cortex

CNS stem cells isolated from the E13–14 cortex have been shown to proliferate in response to bFGF under serum-free culture conditions to give rise to clonal aggregates of undifferentiated neural precursors, called neurospheres (Reynolds & Weiss, 1992; Vescovi *et al.* 1993). The nature of the cells in the bFGF-generated neurospheres was determined by dissociating and seeding the cells at 1 × 10^4 cells cm^{-2} onto poly-L-ornithine–fibronectin-coated glass coverslips and processing them for immunocyto-chemistry 1 h after plating (Fig. 1*D*–*G*). Virtually all of the attached cells were immunoreactive for the neuroepithelial antigen nestin and positive for BrdU. Quantitative analysis revealed that more than 95 % of the total number of BrdU-positive cells were nestin-positive (a total of 217 cells were counted in four independent experiments). These results indicate that the cells in the spheres were undifferentiated

CNS stem cells. Withdrawal of the mitogenic effect of bFGF was shown to initiate the differentiation of CNS stem cells into neurones, astrocytes and oligodendrocytes (Johe *et al.* 1996). To examine whether undifferentiated cells in the neurospheres could differentiate into neurones and astrocytes, the cells were dissociated from the spheres by trituration and were seeded at 1×10^4 cells cm^{-2} onto poly-L-ornithine–fibronectin-coated glass coverslips. bFGF
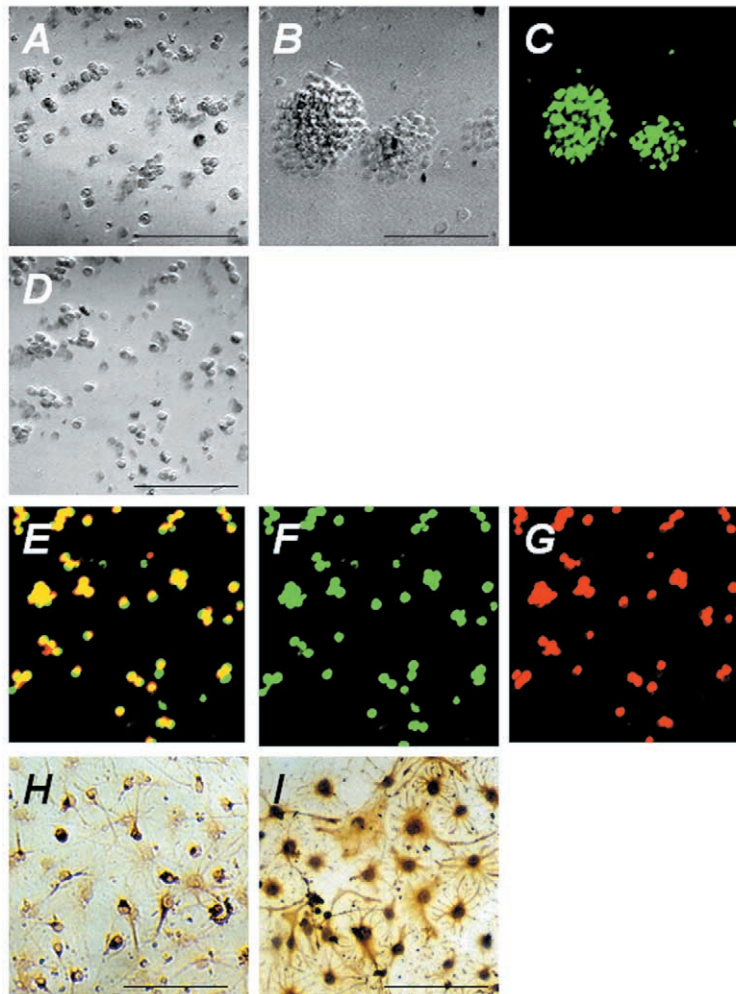

Figure 1. Undifferentiated cells isolated from embryonic rat cortex proliferated in response to basic fibroblast growth factor (bFGF), were immunoreactive for nestin and differentiated into neurones and astrocytes

A, cells isolated from embryonic day 14 (E14) cortex cultured at clonal density in the presence of 10 ng ml^{-1} bFGF underwent cell division after 1 day in culture (phase contrast). Proliferation continued, and after 2 days small clusters of proliferating cells had formed. By 3 days, the clusters had increased in size to give rise to neurospheres (*B*). The spheres were processed for immunocytochemistry with a monoclonal antibody raised against nestin, followed by R-phycoerythrin (R-PE)-conjugated anti-rabbit IgG antibody (*C*: green). To assess the proliferation of central nervous system (CNS) stem cells, the cells were pulsed with 5-bromo-2′-deoxyuridine (BrdU) for 18 h and plated at 1×10^4 cells cm^{-2} onto poly-L-ornithine–fibronectin-coated glass coverslips (*D*: phase-contrast). The cells were fixed and processed for double-labelled immunocytochemistry using anti-BrdU antibody and anti-nestin polyclonal antibody, followed by fluorescein-conjugated anti-mouse antibody and R-PE-conjugated anti-rabbit antibody (yellow in *E*, BrdU + nestin; green in *F*, BrdU; red in *G*, nestin). Virtually all of the BrdU-labelled cells (*E*, *F*) were immunoreactive for nestin (*E*, *G*). bFGF expansion was continued for 1 day before induction of differentiation using 1 % fetal bovine serum (FBS) and bFGF withdrawal. Undifferentiated CNS stem cells were then cultured for 7 days with 1 % FBS after bFGF withdrawal. The cells were fixed and processed for immunocytochemistry using anti-MAP-2 monoclonal antibody and anti-glial fibrillary acidic protein (GFAP) polyclonal antibody, followed by biotinylated anti-mouse and anti-rabbit IgG secondary antibodies. Immunocytochemistry revealed that the differentiated cells showed MAP-2 (*H*) and GFAP (*I*) immunoreactivities. Scale bars in *A*, *B*, *D*, *H* and *I* represent 100 μm.

expansion was continued for 1 day before induction of differentiation by 1% FBS and withdrawal of bFGF. Undifferentiated CNS stem cells were then cultured for 7 days with 1% FBS after the bFGF withdrawal. Immunocytochemistry revealed that the cells expressed MAP-2 and GFAP immunoreactivities (Fig. 1*H*, *I*), indicating that under these conditions the cells readily differentiated into neurones and astrocytes.

CNS stem cells differentiate into smooth-muscle-like cells at low density

CNS stem cells, which normally give rise to neurones, astrocytes and oligodendrocytes under high-density culture conditions, have been shown to differentiate almost exclusively into smooth-muscle-like cells that express α-smooth-muscle actin, SM-22 and basic calponin at low density (Tsai & McKay, 2000). CNS stem cells were cultured at various cell densities as described in Methods. Undifferentiated CNS stem cells were then cultured for 7 days with 10% FBS after bFGF withdrawal. After differentiation, virtually all of the cells at the highest density (1×10^5 cells cm^{-2}) were immunoreactive for GFAP, whereas no α-smooth-muscle-actin-immunoreactive cells were detected (Fig. 2*A*, *D*). Decreasing the cell density decreased the number of GFAP-immunoreactive cells with a concomitant increase in α-smooth-muscle-actin-immunoreactive cells. All of the cells at low density (2.5×10^3 cells cm^{-2}) were immunoreactive for α-smooth muscle actin ($\geqslant 99\%$ of the total population), but not for GFAP (Fig. 2*C*, *F*). Most of the cells at low density displayed a flattened morphology and contained α-smooth-muscle-actin-labelled stress fibres.
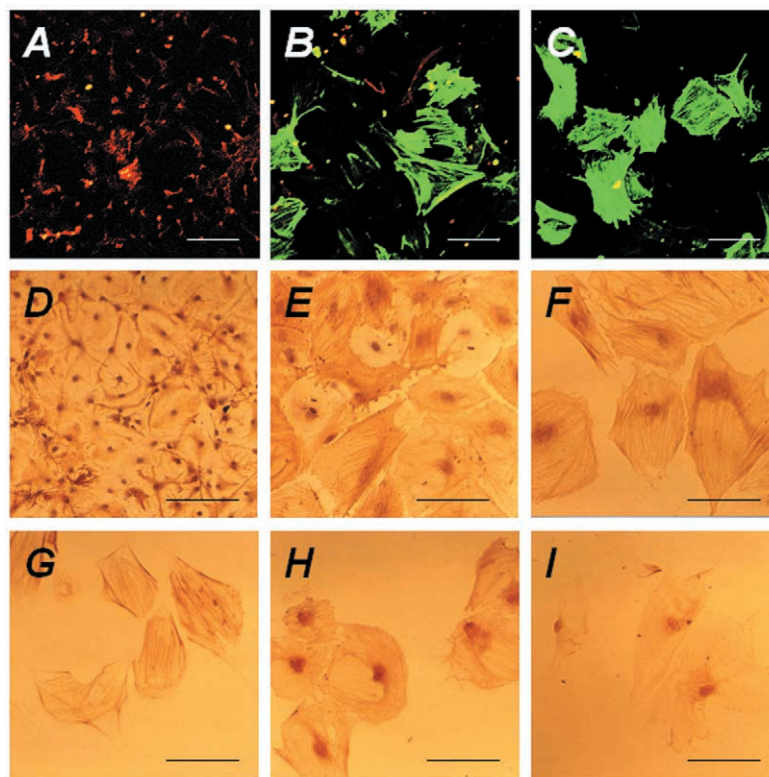

Figure 2. CNS stem cells differentiate into smooth-muscle-like cells at low density

CNS stem cells were cultured on poly-L-ornithine–fibronectin-coated glass coverslips at various cell densities as described in Methods. Undifferentiated CNS stem cells were then cultured for 7 days with 10% FBS after bFGF withdrawal. After differentiation, the cultures were subjected to immunocytochemistry. *A–C*, anti-GFAP and anti-α-smooth-muscle actin antibodies followed by secondary antibodies conjugated to R-PE (red; for GFAP) or fluorescein (green; for α-smooth muscle actin) were used for double-labelling immunocytochemistry, respectively. *D–I*, cells were incubated with anti-GFAP (*D*), anti-α-smooth muscle actin (*E*, *F*), anti-SMemb (*G*), anti-SM-1 (*H*) and anti-SM-2 (*I*), followed by biotinylated anti-mouse secondary antibodies. Virtually all of the cells at the highest density (1×10^5 cells cm^{-2}) were immunoreactive for GFAP (red in *A* and *D*), whereas no α-smooth-muscle-actin-immunoreactive cells were detected (*A*). Decreasing the cell density to 5×10^3 cells cm^{-2} decreased the number of GFAP-immunoreactive cells, with a concomitant increase in the number of α-smooth-muscle-actin-immunoreactive cells (*B*, *E*). All of the cells at low density (2.5×10^3 cells cm^{-2}) were immunoreactive for α-smooth muscle actin (green in *C*, *F*), SMemb (*G*), SM-1 (*H*) and SM-2 (*I*) myosin heavy chains, but not for GFAP (red in *C*, *F*). Most of the cells at low density displayed a flattened morphology and α-smooth-muscle-actin-labelled stress fibres (*F*). Scale bars represent 100 μm.

Table 1. Polymerase chain reaction primers

		Sequence (5′–3′)	Product size (bp)	Annealing temperature (°C)	Reference
GAPDH	Sense	ATCACCATCTTCCAGGAGCG	490	58.5	Law *et al.* (1999)
	Antisense	TAGGAACACGGAAGGCCATG			
α-Smooth-muscle actin	Sense	GATCACCATCGGGAATGAACGC	389	57.5	Park *et al.* (1997)
	Antisense	CTTAGAAGCATTTGCGGTGGAC			
SM-22	Sense	TGTTCCAGACTGTTGACCTC	369	54.9	Tsai & McKay (2000)
	Antisense	GTGATACCTCAAAGCTGTCC			
Basic calponin	Sense	ACAAAAGGAAACAAAGTCAAT	396	55.1	GenBank D14437
	Antisense	GGGCAGCCCATACACCGTCAT			
SM-1/SM-2 myosin heavy chains	Sense	AAGCAGCTCAAGAGGCAG	178 (SM-1)	57	Low *et al.* (1999)
	Antisense	AAGGAACAAATGAAGCCTCGTT	217 (SM-2)		
Nestin	Sense	GGAGTGTCGCTTAGAGGTGC	262	57.3	Law *et al.* (1999)
	Antisense	CAGCAGAGTCCTGTATGTAGCC			
Muscarinic m1 receptor	Sense	GCACAGGCACCCACCAAGCAG	373	60.7	Wei *et al.* (1994)
	Antisense	AGAGCAGCAGCAGGCGGAACG			
Muscarinic m2 receptor	Sense	CACGAAACCTCTGACCTACCC	686	56.5	Wei *et al.* (1994)
	Antisense	TCTGACCCGACGACCCAACTA			
Muscarinic m3 receptor	Sense	GTCTGGCTTGGGTCATCTCCT	434	57.4	Wei *et al.* (1994)
	Antisense	GCTGCTGCTGTGGTCTTGGTC			
Muscarinic m4 receptor	Sense	TGGGTCTTGGCCTTTGTGCTC	588	59.1	Wei *et al.* (1994)
	Antisense	TTCATTGCCTGTCTGCTTTGTTA			
Muscarinic m5 receptor	Sense	CTGGTCTCCTTCATCCTCTGG	394	57.6	Wei *et al.* (1994)
	Antisense	CCTGGGTTGTCTTTCCTGTTG			
Endothelin type A receptor	Sense	TTCGTCATGGTACCCTTCGA	546	54	Kimura *et al.* (1999)
	Antisense	GATACTCGTTCCATACATGG			
Endothelin type B receptor	Sense	TTCACCTCAGCAGGATTCTG	475	54	Kimura *et al.* (1999)
	Antisense	AGGTGTGGAAAGTTAGAACG			
L-type Ca^{2+} channel	Sense	CAGAGCTGCCTCTTCAAAATCGC	437	57	Zeng *et al.* (1999)
	Antisense	ATTCAGGGCAATCTTCCCAAATACC			
N-type Ca^{2+} channel	Sense	AAGAATGTCTTGAACATCCTGATCG	671	57	Zeng *et al.* (1999)
	Antisense	CAGCATCAGCTCGTACTCATAAGG			

To examine further the nature of the differentiated cells, we examined the expression of several additional smooth-muscle-specific proteins by immunocytochemistry and RT-PCR. Immunocytochemical analyses revealed that the cells were immunoreactive for smooth-muscle-specific marker proteins such as SM-1, SM-2 and SMemb myosin heavy chains (Fig. 2*G*–*I*). RT-PCR experiments also indicated the presence of mRNAs for smooth-muscle-specific marker proteins such as SM22, α-smooth-muscle actin, SM-1, SM-2 and basic calponin in differentiated cells (Fig. 3). The cells expressed nestin to a lesser extent than CNS stem cells. These results indicate the smooth-muscle fate of CNS stem cells at low density.

Collagen gel fibre reconstituted with CNS stem-cell-derived smooth-muscle-like cells

To examine whether smooth-muscle-like cells that are differentiated from CNS stem cells possess the characteristics of contractile smooth muscle, we prepared reconstituted collage gel fibres. Reconstituted fibres were prepared by thermal gelation of collagen and smooth-muscle-like cells that had differentiated from CNS stem cells at low density (2.5×10^3 cells cm^{-2}). Within a day

after casting of the gel, the cells contracted and formed a thin fibre spanning the two poles to the bottom of the rectangular wells (Fig. 4*A*). At the same time, astrocytes that had differentiated from CNS stem cells at high density (1×10^5 cells cm^{-2}) were suspended in ice-cold collagen solution. The suspension was poured into a trough and placed in a CO_2 incubator at 37 °C. The gelled preparation was incubated in N2 medium with 10 % FBS for 3 days. The collagen gel containing CNS stem-cell-derived astrocytes contracted to a lesser extent than that containing the smooth-muscle-like cells. Measurement of the steady-state tension generated during formation of the fibres showed that the collagen gel containing CNS stem-cell-derived smooth muscle cells developed a steady-state tension of ~2.8 mN after 1 day of incubation, whereas the gel containing CNS stem-cell-derived astrocytes developed tension to a much smaller extent ($\leqslant$ 0.2 mN). To evaluate the organization of cells populating in the fibre, cells were stained with haematoxylin-eosin. Cells were randomly dispersed when the collagen-cell suspension was cast (Fig. 4*B*). One day after casting, the cells in the fibre exhibited an elongated bipolar spindle shape and were

oriented parallel to the direction of the isometric axis. RT-PCR analysis revealed that the pattern of expression of smooth-muscle-cell marker proteins in reconstituted fibres closely resembled that of the collagen-cell suspension except for a moderate decrease in the expression of these proteins in the fibres (Fig. 4C). A similar decrease in the expression of some smooth-muscle marker proteins was observed with the reconstituted fibres of stomach smooth muscle cells (Oishi *et al.* 2000). It is worth noting that the mRNA for nestin had almost exclusively disappeared in the fibres that had been incubated for 1 day, indicating that the decrease in mRNA for these smooth-muscle-cell marker proteins during the 1 day incubation did not result in a de-differentiation into CNS stem cells.

Tension development and agonist-stimulated contraction

After 1 day of incubation in a CO_2 incubator at 37 °C, the isometric contraction of the fibres was studied (Fig. 5A). Figure 5Aa shows representative contractile responses of the fibres to 80 mM KCl-induced depolarization, which were characterized by a sustained increase in tension. The KCl-induced contraction is considered to result from depolarization of membranes and an increase in trans-membrane influxes of Ca^{2+} via voltage-dependent Ca^{2+} channels. ACh (100 μM) also induced tonic contractions (Fig. 5Ab). Tonic contractions of similar magnitude were triggered by 10 nM endothelin-1 and 10 nM endothelin-2 (Fig. 5Ac, Ad). Prostaglandin F2α (100 μM) also induced tonic contraction. The adrenoceptor stimulant nor-adrenaline (100 μM) did not evoke much of a contractile response (Fig. 5Af). 5-HT (100 μM) as well as angiotensin II (100 μM) also caused little by way of a contractile response (Fig. 5Ag, h). Adenosine (100 μM) caused a slight decrease in tension (Fig. 5Ai). Cumulative dose–response curves demonstrated dose–response relationships for ACh *versus* force (Fig. 5B). The muscarinic antagonist atropine, at a concentration that induced muscarinic receptor-blocking activity (100 nM), inhibited ACh-induced contraction (Fig. 5C).

Contractile properties

To clarify whether the characteristics of contraction of these fibres reflect typical contractile properties of natural smooth muscle tissues, we first studied the effects of a myosin light chain kinase (MLCK) inhibitor, a Rho kinase inhibitor, db-cAMP and 8-Br-cGMP on ACh-induced contraction (Fig. 6). The ACh-induced contraction was completely inhibited by addition of the MLCK inhibitor ML-9 (30 μM), suggesting the involvement of myosin phosphorylation catalysed by MLCK (Fig. 6a). ACh-induced contraction was completely abolished by addition of the Rho kinase inhibitor Y-27632 (1 μM), suggesting the involvement of Rho kinase (Fig. 6b). ACh-induced contraction was also inhibited by the addition of db-cAMP (200 μM) (Fig. 6c) and 8-Br-cGMP (200 μM; Fig. 6d),

indicating the presence of relaxation responses to cAMP and cGMP. An inactive analogue of cAMP, adenosine 3′,5′-cyclic monophosphothionate Rp-isomer, at a concentration of 200 μM, did not inhibit the ACh-induced contractions, but rather enhanced them (data not shown). This small enhancement was probably due to its inhibitory effect on cAMP-dependent protein kinase. Similar observations were also obtained for a selective cGMP-dependent protein kinase inhibitor, Rp-8-((4-chlorophenyl)thio)-cGMPS (data not shown).

We next studied the calcium dependence of ACh-induced contraction. These experiments were performed in calcium-free, Hepes-buffered Tyrode solution, and the results are expressed as percentages of the control ACh-induced contraction induced in the presence of 1.8 mM Ca^{2+}, which
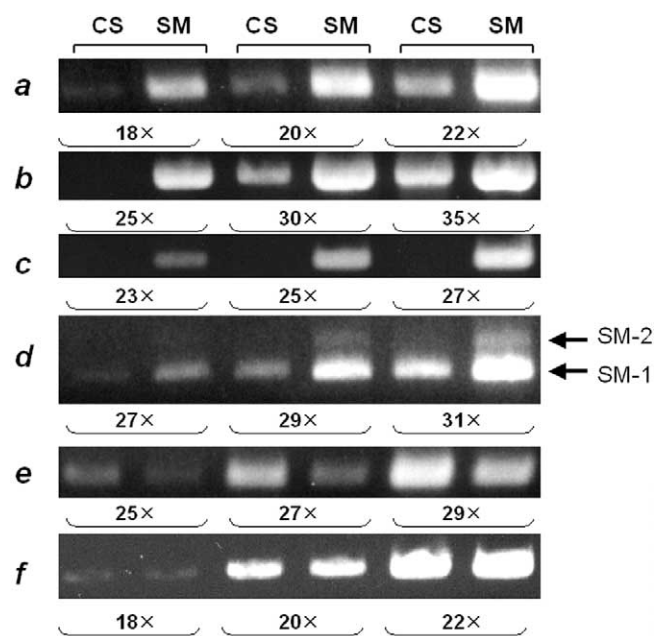

Figure 3. Expression of smooth-muscle-specific proteins at low density

The expression of several smooth-muscle-specific proteins in low-density cultures was examined by semi-quantitative reverse transcriptase-polymerase chain reaction (RT-PCR). CNS stem cells were cultured at low density (2.5×10^3 cells cm^{-2}) as described in Methods. Undifferentiated CNS stem cells were then cultured for 7 days with 10 % FBS after bFGF withdrawal. Total RNAs extracted from CNS stem cells (CS) and the differentiated cells (SM) were subjected to semi-quantitative RT-PCR analysis using primers specific for α-smooth-muscle actin (a), SM-22 (b), basic calponin (c), SM-1/SM-2 myosin heavy chains (d), nestin (e) and GAPDH (f). Results from three consecutive PCR cycles are shown. The PCR products were resolved by electrophoresis on 2 % agarose (3 % in the case of SM-1/SM-2 myosin heavy chains) prestained with ethidium bromide. The results from three consecutive every-other-numbered PCR cycles are shown. The number of PCR cycles is listed at the bottom of each panel. No signal was detected when samples had not been reverse transcribed. Bands at 178 bp (SM-1) and 217 bp (SM-2) were detected with the SM-1/SM-2 primer pair. The PCR primers used are given in Table 1.
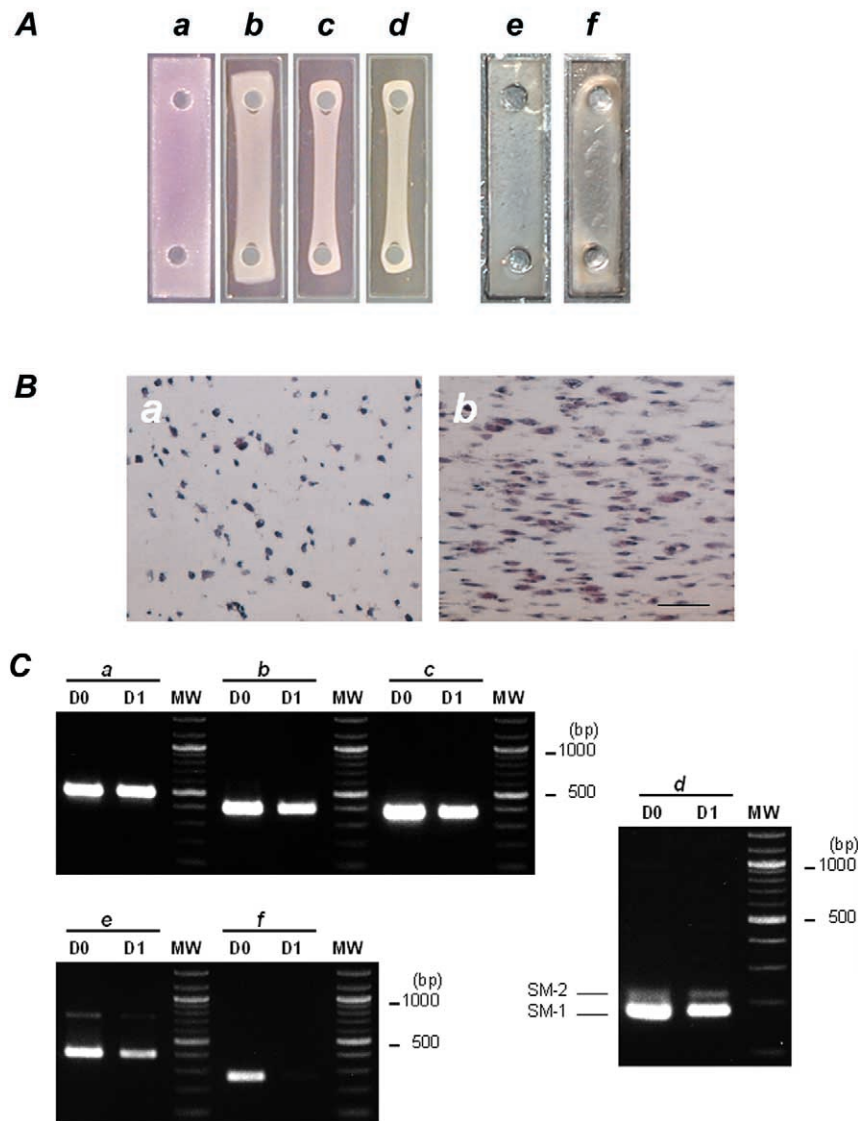
Figure 4. Time-dependent contraction of collagen gels

A, photographs showing time-dependent contraction of collagen gels. A collagen gel suspension containing 2.5×10^6 cells ml^{-1} of CNS stem-cell-derived smooth-muscle-like cells was poured into a rectangular well and placed in a CO_2 incubator at 37 °C in a humidified 5 % CO_2–95 % air atmosphere. The collagen gel suspension gelled within 30 min (*a*). The preparations were incubated in N2 medium in the presence of 10 % FBS for 3 days. Shown are photographs of the gel suspension after 8 h (*b*), 1 day (*c*) and 3 days of incubation (*d*). One day after gels were cast, the diameter of the cross-section was markedly reduced and formed a string-shaped fibre. A collagen gel suspension containing 2.5×10^6 cells ml^{-1} of CNS stem-cell-derived astrocytes was incubated for 3 days. *e*, before incubation; *f*, after 3 days incubation. *B*, haematoxylin-eosin staining of longitudinal sections of collagen gels before incubation (*a*) and after 1 day of incubation (*b*). Longitudinal sections were cut using a cryostat and subjected to haematoxylin-eosin staining. Bar indicates 100 μm and represents the direction of the isometric axis. *C*, RT-PCR analysis of total RNAs extracted from collagen gels before incubation (D0) and after 1 day of incubation (D1). RT-PCR was performed as described in Methods using primers specific for GAPDH (*a*), α-smooth muscle actin (*b*), SM-22 (*c*), SM-1/SM-2 myosin heavy chains (*d*), basic calponin (*e*) and nestin (*f*). The number of PCR cycles was as follows: GAPDH, $\times$ 25; α-smooth muscle actin, $\times$ 25; SM-22, $\times$ 27; SM-1/SM-2 myosin heavy chains, $\times$ 35; basic calponin, $\times$ 29; nestin, $\times$ 29. The PCR products were resolved by electrophoresis on 2 % agarose (3 % in the case of SM-1/SM-2 myosin heavy chains) prestained with ethidium bromide. No signal was detected when samples were not reverse transcribed. Bands at 178 bp (SM-1) and 217 bp (SM-2) were detected with the SM-1/SM-2 primer pair. Molecular weight size markers (MW; 100 bp DNA ladder) are in the right lane. The PCR primers used are given in Table 1.
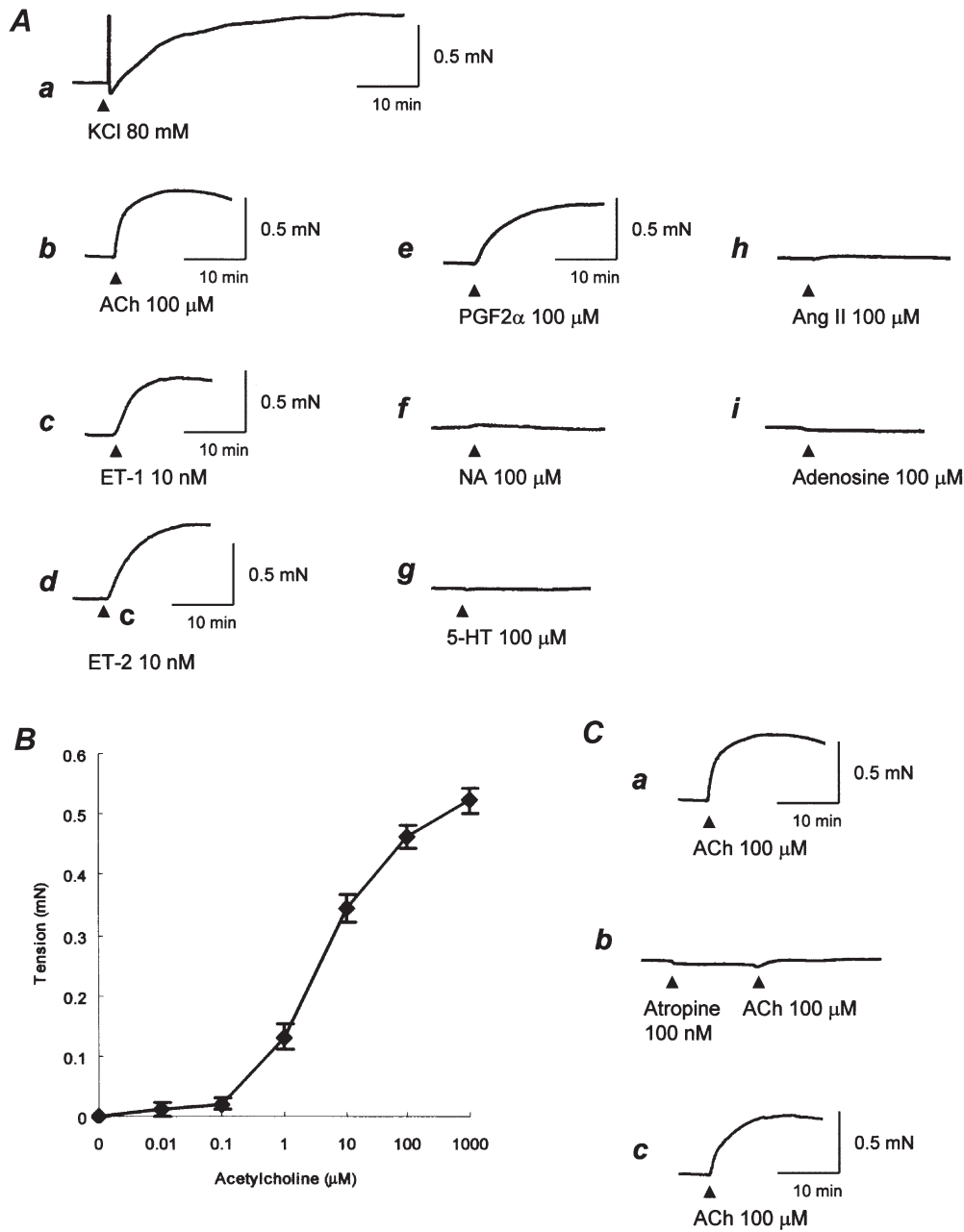
Figure 5. Contractile responses of the fibres to contractile stimulants

A, representative traces showing contractile responses of the fibres to various contractile stimulants. Tension development was recorded isometrically with a force displacement transducer. Contractions were induced by replacing the medium with a potassium-rich solution (*a*) or by adding agonists (*b–i*). *a*, KCl 80 mM; *b*, ACh 100 μM; *c*, endothelin-1 (ET-1) 10 nM; *d*, ET-2 10 nM; *e*, prostaglandin F2α (PGF2α) 100 μM; *f*, noradrenaline (NA) 100 μM; *g*, 5-hydroxytryptamine (5-HT) 100 μM; *h*, angiotensin II (Ang II) 100 μM; *i*, adenosine 100 μM. The maximal tensions produced by KCl, ACh, ET-1, ET-2 and PGF2α were 0.55, 0.53, 0.48, 0.56 and 0.47 mN, respectively. Data are representative traces of repeated experiments (*n* = 4). *B*, dose–response relationships for ACh *versus* force. Contraction was induced by adding ACh cumulatively to achieve the final desired concentration. The points and bars are means ± S.E.M. (*n* = 4). *C*, representative tracings showing atropine-induced inhibition of ACh-induced contraction. The first contraction was induced by adding 100 μM ACh (*a*). The fibre was then washed for 60 min and treated with 100 nM atropine for 10 min. The second contraction was induced by adding 100 μM ACh (*b*). The fibre was again washed for 60 min and then the third contraction was induced likewise (*c*). Representative traces of repeated experiments (*n* = 4).

was elicited at the beginning of the experiment. When the external solution was changed to calcium-free solution (with 1 mM BAPTA) and ACh was added, the ACh-induced contraction was decreased to $55.3 \pm 4.5\%$ ($n = 4$) of the control value, indicating that the contraction was partially dependent upon extracellular Ca^{2+} (Fig. 7*A*). When the fibres were pretreated with 50 μM BAPTA-AM for 15 min in calcium-free solution, the ACh-induced contraction was decreased further to $34.1 \pm 3.7\%$ ($n = 4$), indicating that the intracellular Ca^{2+} chelator BAPTA-AM is partially able to inhibit those parts of the contraction that are independent of extracellular Ca^{2+}. Moreover, the ACh-induced contraction in the presence of Ca^{2+} was partially inhibited ($59.6 \pm 6.2\%$ of control, $n = 4$) by the L-type Ca^{2+} channel inhibitor nifedipine (3 μM), suggesting the involvement of L-type voltage-dependent Ca^{2+} channels (Fig. 7*B*). Finally, the expression of several contractile agonist receptors and voltage-dependent Ca^{2+} channels in the collagen gel fibres was examined by RT-PCR. The differentiated cells in the fibres expressed all of the muscarinic ACh receptor m1–m5 subtypes, endothelin type A and B receptors, and L-type and N-type voltage-dependent Ca^{2+} channels.

DISCUSSION

We have developed a reconstituted hybrid fibre of smooth-muscle-like cells that differentiated from CNS stem cells, which permits for the first time direct measurement of the contractile forces generated by these cells. The present method allows further investigation of the molecular mechanisms underlying the differentiation and contractile function of CNS stem-cell-derived smooth-muscle-like cells.

Mature smooth muscle cells are terminally differentiated cells that express smooth-muscle-specific marker proteins such as α-smooth-muscle actin, SM-22, basic calponin and smooth muscle myosin heavy chains. Alpha-smooth-muscle actin is expressed exclusively by smooth muscle cells and smooth-muscle-related cells such as pericytes and juxtaglomerular cells. However, its expression alone does not provide definitive evidence for a smooth muscle cell lineage (Owens, 1995). It is known that α-smooth-muscle actin is expressed transiently in the early stages of differentiation of both cardiac and skeletal myocytes (Ruzicka & Schwartz, 1988; Woodcock-Mitchell *et al.* 1990), myofibroblasts (Darby *et al.* 1991) and tumour cells (Cintorino *et al.* 1991). In this study, we observed that stimulation of CNS stem cells by FBS in a low-density culture effectively induced differentiation to express SM-22 and basic calponin in addition to α-smooth-muscle actin, supporting the earlier findings of Tsai & McKay (2000). Moreover, these smooth-muscle-like cells also expressed differentiated smooth-muscle-cell marker proteins, SM-1 and SM-2 myosin heavy chains, and a developing smooth-muscle-cell marker protein, SMemb myosin heavy chain. These results suggest that the smooth-muscle-like cells express some smooth muscle marker proteins that are typically considered to be
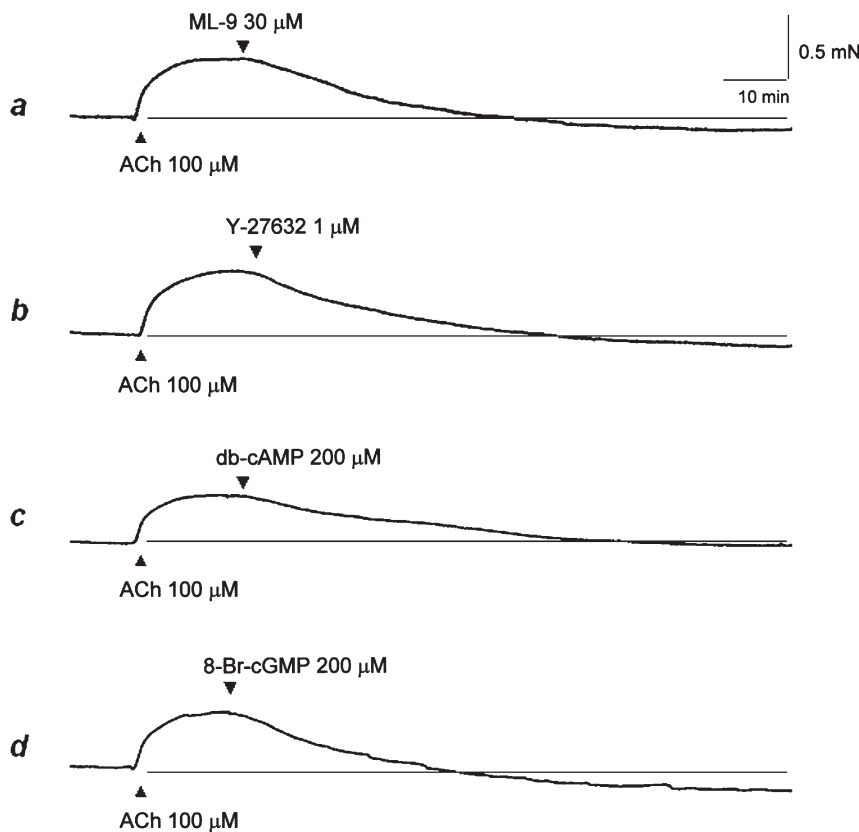

Figure 6. Representative tracing showing inhibition of ACh-induced contraction by ML-9 (*a*), Y-27632 (*b*), dibutyryl cAMP (db-cAMP; *c*) and 8-bromo-cGMP (8-Br-cGMP; *d*)

The contraction was induced by adding 100 μM ACh, then 30 μM ML-9, 1 μM Y-27632, 200 μM db-cAMP and 200 μM 8-Br-cGMP was applied 8–10 min later. Representative traces of repeated experiments ($n = 4$).

indicative of a smooth muscle contractile phenotype, including SM-1 and SM-2 myosin heavy chains.

The primary function of smooth muscle cells in mature animals is contraction. To examine whether these CNS stem-cell-derived smooth-muscle-like cells have a typical contractile function identical to the smooth muscle *in vivo*, we used the method of reconstituting hybrid fibres. This technique allows the functional study of a variety of smooth muscle cells undergoing biochemical and genetic manipulations. It has been reported that cultured smooth muscle cells inoculated into collagen gels shrink spontaneously with time because of cellular traction (Tomasek *et al.* 1982). When the spontaneous contraction was mechanically restricted, smooth muscle cells in gels exhibited an elongated bipolar spindle shape and were oriented parallel to the direction of stretching (Oishi *et al.* 2000). In the study presented here, collagen gel suspensions containing CNS stem-cell-derived smooth-muscle-like cells were poured into a rectangular well with two poles on the bottom and were incubated in N2 medium in the presence of 10 % FBS. The cells shrank the gel and formed a string-shaped fibre. The cells in fibres that were incubated for 1 day exhibited an elongated bipolar spindle shape and were oriented parallel to the

direction of the isometric axis. In contrast, CNS stem-cell-derived astrocytes caused collagen gel contraction to a lesser extent than the smooth-muscle-like cells. These results indicate that the smooth-muscle-like cells possess the ability to contract the collagen gel.

Several important observations in the present study suggest that the characteristics of contraction reflect typical smooth muscle contractility. First, isometric force measurements revealed contraction of the fibres in response to KCl-induced depolarization. The fibres also showed contraction in response to potent contractile agonists including endothelin-1, endothelin-2, prostaglandin F2α and ACh. These results indicate that the cells in the fibres exhibit contractile responses to typical contractile stimuli. Second, the fibres responded to typical smooth muscle relaxants such as db-cAMP and 8-Br-cGMP. Smooth muscle relaxation is supposed to be mediated by intracellular cAMP and cGMP (Toda & Okamura, 1998). These findings suggest strongly that typical relaxation mechanisms are maintained in the
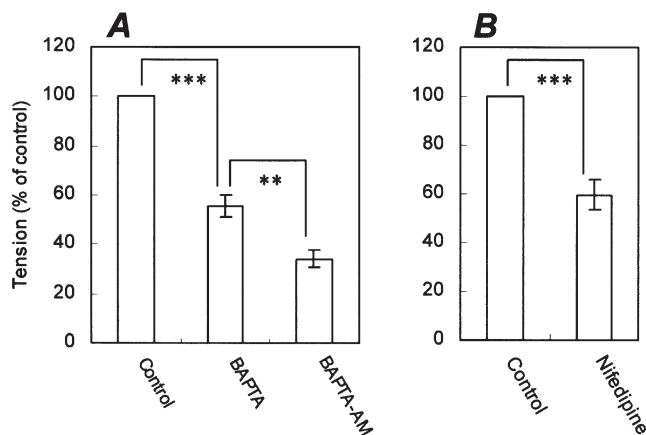

Figure 7. Calcium dependence of contraction and its inhibition by nifedipine

A, the first contraction was induced by adding 100 μM ACh (control) in normal Hepes-buffered Tyrode solution. The fibre was then washed for 60 min with calcium-free, Hepes-buffered Tyrode solution. The second contraction was induced by adding 100 μM ACh in calcium-free solution in the presence of 1 mM BAPTA, an extracellular Ca^{2+} chelator (BAPTA). The fibre was then washed for 60 min with calcium-free solution and treated with 50 μM BAPTA-AM, an intracellular Ca^{2+} chelator. The third contraction was induced by adding 100 μM ACh (BAPTA-AM). *B*, the first contraction was induced by adding 100 μM ACh (control). The fibre was then washed for 60 min and treated with 3 μM nifedipine for 10 min. The second contraction was induced by adding 100 μM ACh (nifedipine). The data are expressed as percentages of the first contraction. Bars represent means ± S.E.M. (*n* = 4). **$P \leqslant 0.01$; ***$P \leqslant 0.005$, compared between groups.
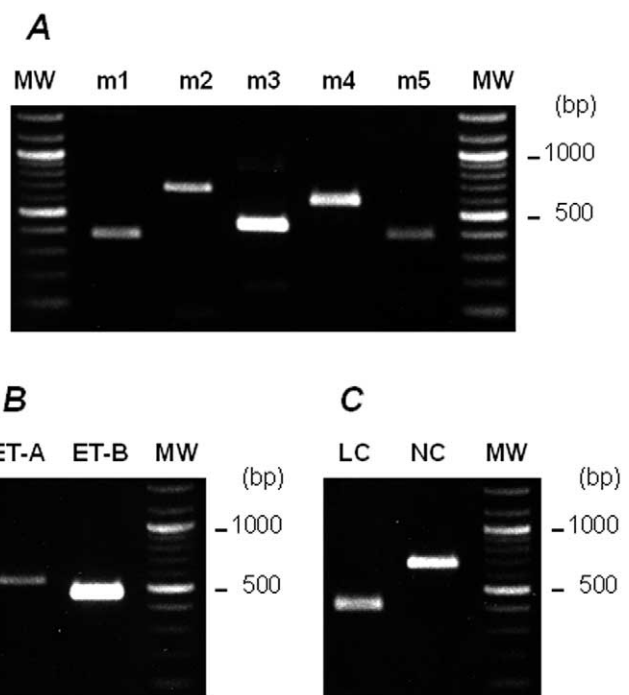

Figure 8. Expression of several contractile agonist receptors and voltage-dependent Ca^{2+} channels in the collagen gel fibres, as examined by RT-PCR

RT-PCR was performed as described in Methods using primers specific for muscarinic ACh receptor subtypes m1–m5 (*A*), endothelin receptor subtypes ET-A and ET-B (*B*), and L-type (LC) and N-type (NC) Ca^{2+} channels (*C*). The number of PCR cycles was as follows: m1, × 35; m2, × 35; m3, × 35; m4, × 35; m5, × 35; ET-A, × 30; ET-B, × 30; LC, × 35; NC, × 35. The PCR products were resolved by electrophoresis on 2 % agarose prestained with ethidium bromide. No signal was detected when samples were not reverse transcribed. MW, molecular weight size markers (100 bp DNA ladder). The PCR primers used are given in Table 1.

reconstituted fibres. Third, the contraction was dependent upon Ca^{2+}. The removal of extracellular Ca^{2+} resulted in a decrease in the force induced by ACh. A similar decrease in the force was observed when the fibre was pretreated with the L-type Ca^{2+} channel inhibitor nifedipine and then stimulated with ACh in calcium-containing medium. RT-PCR analysis of total RNA isolated from the smooth muscle fibres, using sequence-specific oligonucleotide primers designed with reference to the published sequence of the rat voltage-dependent Ca^{2+} channel α-subunit genes, revealed that mRNA for L-type as well as N-type Ca^{2+} channels was present in the fibres. These results suggest strongly that Ca^{2+} entry from extracellular sources, primarily through nifedipine-sensitive, voltage-dependent Ca^{2+} channels, causes the increase in contractile force induced by ACh. This was supported by the finding that KCl-induced depolarization of the smooth muscle cell membrane caused significant force development. Taken together, these results suggest that Ca^{2+} entry through nifedipine-sensitive, voltage-dependent Ca^{2+} channels causes an increase in contractile force. The contractions were dependent upon MLCK and Rho kinase. The MLCK inhibitor ML-9 inhibited the contraction evoked by ACh. Furthermore, the ACh-induced contraction was completely inhibited by the highly selective Rho kinase inhibitor Y-27632. These findings suggest strongly that the contraction is regulated by MLCK-dependent and Rho-kinase-dependent mechanisms. The results of the present study show that CNS stem cells differentiate *in vitro* into smooth muscle cells that have a typical contractile function identical to smooth muscle *in vivo*.

Smooth muscle cells, with the exception of vascular smooth muscle cells, are generally believed to be derived from mesoderm. Vascular smooth muscle cells can be derived from an additional source, the neural crest. Gross mapping of the embryological origins of vascular smooth muscle cells has been accomplished using interspecies grafting techniques in which regions of developing embryos from one species are surgically removed and transplanted into a host embryo from another species. The results of these studies have shown that vascular smooth muscle cells are derived from the splanchnic layer of the ventrolateral plate mesoderm (Lelievre & Ledouarin, 1975). An exception to this is the large vessels of the head and neck, which are derived from neural crest mesectodermal cells (Lelievre & Ledouarin, 1975; Hood & Rosenquist, 1992). This exception is by no means unique to smooth muscle cells, in that in the head, many of the neural crest cells will differentiate into cartilage, bone and other connective tissues, which elsewhere in the body arise from the mesoderm.

A recent study using stem cells isolated from rodent E10.5–E13.5 spinal cord (Mujtaba *et al.* 1998) revealed an unexpected differentiation into smooth-muscle-like cells induced by bone morphogenic proteins (BMPs). In these experiments, the CNS stem cells could give rise to a transient p75/nestin-immunoreactive neural crest stem-cell-like population, which subsequently differentiated into peripheral neurones, smooth-muscle-like cells and Schwann cells in mass and clonal culture. The study by Mujtaba *et al.* suggested that CNS stem cells could, in the presence of BMP2/4, switch fate to become neural crest stem cells. Based on the results of the present study, it is still not clear whether CNS stem cells can transiently transdifferentiate into neural crest stem cells and give rise to smooth muscle cells. The question also remains whether CNS stem cells adopt the smooth muscle fate *in vivo* after neural tube closure and, if they do, where they reside and what their physiological functions are. These issues need to be clarified in future studies.

Although the significance of the CNS stem cell origin of smooth muscle cells in physiological and pathological states needs to be evaluated, these observations suggest that smooth muscle cells are in part derived from CNS stem cells. It is also currently unknown which parts of smooth muscles are derived from CNS stem cells. One likely candidate would be the cerebral blood vessels. In support of this, our results indicate that responses to agonists were similar to those of cerebral arteries. The fibres responded to several contractile agonists including endothelin-1, endothelin-2, prostaglandin F2α and ACh. It has been demonstrated that endothelin and prostaglandin F2α induce vasoconstriction in cerebral arteries (Toda & Okamura, 1993; Petersson *et al.* 1996). Endothelin-1 plays roles in the maintenance of cerebral vascular tone as well as in the pathogenesis of cerebral vasospasm (Goto *et al.* 1996). An endothelin receptor subtype, ET-A, is involved in endothelin-1-induced vasoconstriction. Recent findings indicate that another endothelin receptor subtype ET-B receptor also modulates constriction (White *et al.* 1998; Hansen-Schwartz & Edvinsson, 2000). In support of this, RT-PCR experiments indicate the presence of mRNAs for both endothelin receptor subtypes ET-A and ET-B in the fibres.

NA is known to be a potent vasoconstrictor. The extent of NA-induced vasoconstriction was, however, markedly less in the cerebral arteries than seen in extracerebral arteries (Toda, 1983; Hogestatt & Andersson, 1984). Consistent with this, we found that NA induced little contractile response in the fibres. In contrast, ACh elicited contraction of the fibres. It is well known that ACh is an important regulator of local cerebral blood flow (Dauphin & MacKenzie, 1995; Sato & Sato, 1995). Some cerebrovascular smooth muscles exhibit two different muscarinic vasomotor responses, endothelium-dependent relaxation and endothelium-independent contraction (Edvinsson *et al.* 1977; Dauphin

et al. 1991). Intraparenchymal smooth muscle cells of microvessels exhibited messages for all except the m4 muscarinic ACh receptor subtype (Elhusseiny *et al.* 1999). In the present study, RT-PCR experiments indicated the presence of mRNAs for all of the muscarinic ACh receptor subtypes, ET-A and ET-B receptors, and L-type and N-type voltage-dependent Ca^{2+} channels in the fibres. Adenosine is a potent cerebral vasodilator (Wahl & Kuschinsky, 1976). Brain adenosine concentrations have been found to increase under conditions of ischaemia. Adenosine A2A receptor antagonists have proved to be active in models of cerebral ischaemia. In the present study, adenosine caused a slight decrease in tension. Taken together, these results support the possibility that cerebral blood vessels are derived from CNS stem cells, although the precise biological functions of CNS stem cells remain to be clarified.

Our results, as well as previous findings by Tsai & McKay (2000), suggest that the fate of smooth muscle cells, astrocytes and neurones can be acquired directly from common CNS stem cells. Palmer *et al.* (2000) reported that both neurogenesis and angiogenesis occurred within a tight proliferative cluster associated with the microvasculature of the hippocampus subgranule zone. These proliferative clusters consisted of neural precursors, committed neuroblasts, glia and endothelial precursors. Although endothelial cells can initiate angiogenesis, the subsequent vascular myogenesis is important to promote functional new blood vessels; vessels become covered by smooth muscle cells. Indeed, vessels regress easily as long as they are not covered by smooth muscle cells. Leventhal *et al.* (1999) showed that the brain microvascular endothelium promotes the survival and differentiation of neural precursors (perhaps CNS stem cells). Therefore, the possibility arises that CNS-specific vascular myogenesis may recruit these smooth muscle cells that are derived from the CNS stem cells associated with the microvasculature bed in response to circulating factors.

In conclusion, multipotent stem cells in the CNS were isolated from rat E14 cortex and shown to differentiate into smooth-muscle-like cells. To examine whether these smooth-muscle-like cells possess characteristics of contractile smooth muscle, collagen gel fibres were prepared. The fibres contracted in response to KCl-induced depolarization and typical contractile agonists. ACh-induced contraction was partially inhibited by nifedipine and the intracellular Ca^{2+} chelator BAPTA-AM, and abolished by MLCK and Rho kinase inhibitors, db-cAMP and 8-Br-cGMP. These results suggest that *in vitro* CNS stem cells give rise to smooth muscle cells that have an identical contractile function to smooth muscle *in vivo*, raising the possibility that smooth muscle cells are in part derived from CNS stem cells.

REFERENCES

Cintorino, M., Bellizzi De Marco, E., Leoncini, P., Tripodi, S. A., Xu, L. J., Sappino, A. P., Schmitt-Graff, A. & Gabbiani, G. (1991). Expression of alpha-smooth-muscle actin in stromal cells of the uterine cervix during epithelial neoplastic changes. *International Journal of Cancer* **47**, 843–846.

Darby, I., Skalli, O. & Gabbiani, G. (1991). Alpha-smooth muscle actin is transiently expressed by myofibroblasts during experimental wound healing. *Laboratory Investigation* **63**, 21–29.

Dauphin, F. & MacKenzie, E. T. (1995). Cholinergic and vasoactive intestinal polypeptidergic innervation of the cerebral arteries. *Pharmacology and Therapeutics* **67**, 385–417.

Dauphin, F., Ting, V., Payette, P., Dennis, M. & Hamel, E. (1991). Vasocontractile muscarinic M1 receptors in cat cerebral arteries: pharmacological identification and detection of mRNA. *European Journal of Pharmacology* **207**, 319–327.

Edvinsson, L., Falck, B. & Owman, C. (1977). Possibilities for a cholinergic action on smooth musculature and on sympathetic axons in brain vessels mediated by muscarinic and nicotinic receptors. *Journal of Pharmacology and Experimental Therapeutics* **200**, 117–126.

Elhusseiny, A., Cohen, Z., Olivier, A., Stanimirovic, D. B. & Hamel, E. (1999). Functional acetylcholine muscarinic receptor subtypes in human brain microcirculation: identification and cellular localization. *Journal of Cerebral Blood Flow and Metabolism* **19**, 794–802.

Goto, K., Hama, H. & Kasuya, Y. (1996). Molecular pharmacology and pathophysiological significance of endothelin. *Japanese Journal of Pharmacology* **72**, 261–290.

Gritti, A., Parati, E. A. A, Cova, L., Frolichsthal, P., Galli, R., Wanke, E., Faravelli, L., Morassutti, D. J., Roisen, F., Nickel, D. D. & Vescovi, A. L. (1996). Multipotential stem cells from the adult mouse brain proliferate and self-renew in response to basic fibroblast growth factor. *Journal of Neuroscience* **16**, 1091–1100.

Hansen-Schwartz, J. & Edvinsson, L. (2000). Increased sensitivity to ET-1 in rat cerebral arteries following organ culture. *NeuroReport* **28,** 649–652.

Hogestatt, E. D. & Andersson, K. E. (1984). On the postjunctional alpha-adrenoreceptors in rat cerebral and mesenteric arteries. *Journal of Autonomic Pharmacology* **4**, 161–173.

Hood, L.C. & Rosenquist, T. H. (1992). Coronary artery development in the chick: origin and deployment of smooth muscle cells, and the effects of neural crest ablation. *Anatomical Record* **234**, 291–300.

Johe, K. K., Hazel, T. G., Muller, T., Dugich-Djordjevic, M. M. & McKay, R. D. (1996). Single factors direct the differentiation of stem cells from the fetal and adult central nervous system. *Genes and Development* **10**, 3129–3140.

Kimura, A., Ohmichi, M., Takeda, T., Kurachi, H., Ikegami, H., Koike, K., Masuhara, K., Hayakawa, J., Kanzaki, T., Kobayashi, M., Akabane, M., Inoue, M., Miyake, A. & Murata, Y (1999). Mitogen-activated protein kinase cascade is involved in endothelin-1-induced rat puerperal uterine contraction. *Endocrinology* **140**, 722–731.

Law, A. K., Pencea, V., Buck, C. R. & Luskin, M. B. (1999). Neurogenesis and neuronal migration in the neonatal rat forebrain anterior subventricular zone do not require GFAP-positive astrocytes. *Developmental Biology* **216**, 622–634.

Lelievre, C. & Ledouarin, N. (1975). Mesenchymal derivatives of the neural crest: analysis of chimaeric quail and chick embryos. *Journal of Embryology and Experimental Morphology* **34**, 125–154.

Leventhal, C., Rafii, S., Rafii, D., Shahar, A. & Goldman, S. A. (1999). Endothelial trophic support of neuronal production and recruitment from the adult mammalian subependyma. *Molecular and Cellular Neurosciences* **13**, 450–464.

Low, R. B., White, S. L., Low, E. S., Neuville, P., Bochaton-Piallat, M. L. & Gabbiani, G. (1999). Age dependence of smooth muscle myosin expression by cultured rat aortic smooth muscle cells. *Differentiation* **65**, 151–159.

Mujtaba, T., Mayer-Proschel, M. & Rao, M. S. (1998). A common neural progenitor for the CNS and PNS. *Developmental Biology* **200**, 1–15.

Oishi, K., Itoh, Y., Isshiki, Y., Kai, C., Takeda, Y., Yamaura, K., Takano-Ohmuro, H. & Uchida, M. K. (2000). Agonist-induced isometric contraction of smooth muscle cell-populated collagen gel fiber. *American Journal of Physiology – Cell Physiology* **279**, C1432–1442.

Owens, G. K. (1995). Regulation of differentiation of vascular smooth muscle cells. *Physiological Reviews* **75**, 487–517.

Palmer, T. D. Willhoite, A. R. & Gage, F. H. (2000). Vascular niche for adult hippocampal neurogenesis. *Journal of Comparative Neurology* **425**, 479–494.

Park, F., Mattson, D. L., Roberts, L. A. & Cowley, A. W. Jr (1997). Evidence for the presence of smooth muscle alpha-actin within pericytes of the renal medulla. *American Journal of Physiology* **273**, R1742–1748.

Petersson, J., Hanson, G. C., Lindberg, B. F. & Hogestatt, E. D. (1996). Contractile effect of big endothelin-1 and its conversion to endothelin-1 in rabbit cerebral arteries. *Naunyn-Schmiedeberg's Archives of Pharmacology* **354**, 656–661.

Reynolds, B. A. & Weiss, S. (1992). Generation of neurons and astrocytes from isolated cells of the adult mammalian central nervous system. *Science* **255**, 1707–1710.

Ruzicka, D. L. & Schwartz, R. J. (1988). Sequential activation of alpha-actin genes during avian cardiogenesis: vascular smooth muscle alpha-actin gene transcripts mark the onset of cardiomyocyte differentiation. *Journal of Cell Biology* **107**, 2575–2586.

Sato, A. & Sato, Y. (1995). Cholinergic neural regulation of regional cerebral blood flow. *Alzheimer Disease and Associated Disorders* **9**, 28–38.

Toda, N. (1983). Alpha adrenergic receptor subtypes in human, monkey and dog cerebral arteries. *Journal of Pharmacology and Experimental Therapeutics* **226**, 861–868.

Toda, N. & Okamura, T. (1993). Cerebral vasoconstrictor mediators. *Pharmacology and Therapeutics* **57**, 359–375.

Toda, N. & Okamura, T. (1998). Cerebral vasodilators. *Japanese Journal of Pharmacology* **76**, 349–367.

Tomasek, J. J., Hay, E. D. & Fujiwara, K. (1982). Collagen modulates cell shape and cytoskeleton of embryonic corneal and fibroma fibroblasts: distribution of actin, alpha-actinin, and myosin. *Developmental Biology* **92**, 107–122.

Tsai, R. Y. & McKay, R. D. (2000). Cell contact regulates fate choice by cortical stem cells. *Journal of Neuroscience* **20**, 3725–3735.

Vescovi, A. L., Reynolds, B. A., Fraser, D. D. & Weiss, S. (1993). bFGF regulates the proliferative fate of unipotent (neuronal) and bipotent (neuronal/astroglial) EGF-generated CNS progenitor cells. *Neuron* **11**, 951–966.

Wahl, M. & Kuschinsky, W. (1976). The dilatatory action of adenosine on pial arteries of cats and its inhibition by theophylline. *Pflügers Archiv* **362**, 55–59.

Wei, J., Walton, E. A., Milici, A. & Buccafusco, J. J. (1994). m1-m5 muscarinic receptor distribution in rat CNS by RT-PCR and HPLC. *Journal of Neurochemistry* **63**, 815–821.

White, L. R., Leseth, K. H., Juul, R., Adner, M., Cappellen, J., Aasly, J. & Edvinsson, L. (1998). Increased endothelin ETB contractile activity in cultured segments of human temporal artery. *Acta Physiologica Scandinavica* **164**, 21–27.

Woodcock-Mitchell, J., Mitchell, J. J., Low, R. B., Kieny, M., Sengel, P., Rubbia, L., Skalli, O., Jackson, B. & Gabbiani, G. (1990). Alpha-smooth muscle actin is transiently expressed in embryonic rat cardiac and skeletal muscles. *Differentiation* **39**, 161–166.

Zeng, N., Athmann, C., Kang, T., Walsh, J. H. & Sachs, G. (1999). Role of neuropeptide-sensitive L-type Ca^{2+} channels in histamine release in gastric enterochromaffin-like cells. *American Journal of Physiology* **277**, G1268–1280.

Acknowledgements